J. Vac. Sci. Technol. A, Vol. 24, No. 4, 1012 (2006)

Plasma etching of proton-exchanged lithium niobate

H. Hu
Department of Physics, University of Paderborn, D-33095 Paderborn, Germany

A. P. Milenin
Max Planck Institute of Microstructure Physics, Weinberg 2, D-06120 Halle, Germany

R. B. Wehrspohn,[a] H. Hermann, and W. Sohler
Department of Physics, University of Paderborn, D-33095 Paderborn, Germany

(Received 25 January 2006; accepted 26 April 2006; published 9 June 2006)

Plasma etching of lithium niobate with fluorine gases is limited by the redeposition LiF. This results in a low etch rate and nonvertically etched walls. Etching of proton-exchanged lithium niobate can prevent the LiF deposition to a large extent because of the greatly reduced lithium concentration in lithium niobate. We performed different inductively coupled plasma etching processes using SF_6 or CHF_3/Ar on proton-exchanged lithium niobate. Negligible underetching and nearly vertically etched walls on proton-exchanged lithium niobate samples were obtained by CHF_3/Ar gas at chamber pressure of 6 mTorr and 130 V dc bias. © *2006 American Vacuum Society.*
[DOI: 10.1116/1.2207150]

I. INTRODUCTION

Lithium niobate ($LiNbO_3$, LN) is a crystalline dielectric material being of particular interest for integrated optics due to its excellent electro-optical, acousto-optical, and nonlinear optical properties.[1] The realizations of LN ridge waveguide and LN photonic crystal waveguides require anisotropic etching techniques of the LN substrate. Wet etch and dry etching methods are widely used in shaping LN crystals.[2,3] Dry etching is a very controllable process and has the advantage of being highly anisotropic.[4] Plasmas based on fluorine gases are generally used for plasma etching of LN due to the good volatility of fully fluorinated niobium species at temperature about 200 °C. However, one of the main problems of dry etching of LN with fluorine based plasmas is the redeposition of LiF.[5] During the plasma etching of LN, LiF is formed, which has a melting temperature of more than 800 °C. The LiF will redeposit on the surface of the substrate and lower the etching rate. Therefore, it is difficult to obtain vertical etching profiles if redeposition becomes the dominating process. To avoid redeposition of LiF, it is possible to enhance the sputtering process during the etching, for instance, by adding argon in the etching gas.[6] Another possible way is to reduce the lithium concentration in lithium niobate. By a proton exchange (PE) process, lithium ions can be replaced by protons in LN. This is believed to be one-to-one substitution. Depending on the PE parameters, up to 85% of Li ions can be substituted.[7] Thus, plasma etching of PE-LN will have a significant smaller amount of LiF redeposition than that of pure LN, increasing the etching rate and improving the etch profiles. By using the reverse proton exchange process, protons can be substituted by lithium ions.[8] In principle, the plasma-etched PE-LN sample can be reverse proton exchanged to restore the optical properties of LN. Parallel plate reactive ion etching of proton-exchanged LN waveguide was recently performed by Fogeletti *et al.* to fabricate linear gratings.[9] The etching rate was about 0.6 μm/h and the etching depth was about 0.25–0.4 μm. We carried out a detailed study using also inductively coupled plasmas and different fluorine-containing gas mixtures. First photonic crystal waveguide structures have been successfully fabricated with an etch depth of 1.5 μm.

II. EXPERIMENT

Proton exchange of Z-cut LN samples was performed in pure benzoic acid at 240 °C for 5 h. The PE depth was 2.8 μm as determined by optical microscopy of a polished end face. The PE-LN surface was then covered by a 120–400 nm thick Cr layer using sputter deposition. The Cr layer serves as etch mask for the successive plasma-chemical etching process of LN. For the ridge waveguides, Cr stripes of 9.5–19.5 μm width were defined by photolithography. For the photonic crystal waveguides, electron beam lithography has been used with pore diameter of 340 nm and an interpore distance of about 500 nm. The Cr layer was opened for the ridge waveguides by wet etching and for the photonic crystal waveguides by plasma etching using the parameters described in Ref. 10. The etching of LN was performed either in a standard reactive ion etching equipment, Tepla 100-E, or in an Oxford Plasmalab System 100 with ICP 380 source installed in a clean room of class 1. Table I give a summary of the plasma parameters and the etch rate. In experiments 1 and 2, the Tepla parallel plate reactor was used, and in the experiments 3, 4, and 5 the Oxford Plasmalab machine was used in the inductively coupled mode. As-purchased, pure LN samples with Cr stripes having the same parameters were etched together with PE-LN for comparison. After etching, the Cr structure was removed by wet

[a]Author to whom correspondence should be addressed; electronic mail: wehrspohn@physik.upb.de

TABLE I. Dry etching parameters, etching rate, and average selectivity.

No.	Gas and flow rate (SCCM[a])	Power (W)	dc bias (V)	Chamber pressure (mTorr)	Sample cooling	Average etching rate (nm/h)	Average selectivity
1	CF_4	300	⋯	500	No cooling	Pure LN: 157 PE-LN: 480 Cr: 140	Pure LN/Cr=1.12 PE-LN/Cr=3.43
2	SF_6	300	⋯	500	No cooling	Pure LN: cannot be etched PE-LN: 1530 Cr: 33	PE-LN/Cr=46
3	SF_6 50	1500	153	6	He cooling backside	Pure-LN: 450 PE-LN: 2740 Cr ~ 90	Pure LN/Cr ~ 5 PE-LN/Cr ~ 30
4	CHF_3/Ar 50/50	1500	122	6	He cooling backside	Pure LN: 650 PE LN: 2880 Cr ~ 60	Pure LN/Cr ~ 11 PE-LN/Cr ~ 48
5	CHF_3/Ar 50/50	1500	130	6	No cooling	PE-LN: 5760 Cr ~ 180	PE-LN/Cr ~ 32

[a]SCCM denotes standard cubic centimer per minute.

etching. Scanning electron microscopy and optical microscopy were performed to analyze the etch rate and the side walls.

III. RESULTS AND DISCUSSION

The dry etching parameters, etching rates, and selectivity are shown in Table I. In experiments 1 and 2, a high gas pressure ($p=500$ mTorr) was used to test if plasma-chemical etching processes occur on PE-LN. Two different gases were studied: CF_4 and SF_6. With CF_4 at $p=500$ mTorr, the etching rate of PE-LN is 480 nm/h. The etching rate ratio of PE-LN to pure LN is about 3. On the sample surface, there are cracks for the CF_4-etched PE-LN sample [Fig. 1(a)]. With SF_6 gas at $p=500$ mTorr, the etching rate of PE-LN is 1.53 μm/h. A relatively smooth etched surface was observed by optical microscope [Fig. 1(b)]. The etching ratio of PE-LN to Cr is 46. The pure LN was not etched at all, probably due to the redeposition of LiF species.

Parallel plate reactive ion etching at a $p=500$ mTorr is basically an isotropic chemical etching process with almost no physical component. The large etching rate difference between PE-LN and pure LN shows that proton exchange of LN can overcome the formation of LiF to a large extent, in particular, with SF_6, which exhibits an etching ratio between PE-LN and Cr of more than 40. We further investigated sample 2 by optical microscope and scanning electron microscopy (SEM). Figure 2 shows the PE-LN surface etched by SF_6. The Cr stripe covered initially the PE-LN but a part of the Cr layer was taken away to show the underlying nonetched LN stripe (right part of Fig. 2). Due to the highly isotropic etching, a significant underetching of the Cr stripe occurred. On each edge of the stripe, the lateral underetching rates were 3.5 and 4.0 μm/h, respectively. Figure 3 shows the SEM picture of the end facet of PE-LN etched in SF_6. The strongly nonvertical side walls are another indication for a highly isotropic etching process.

In order to obtain vertical side walls and deeper etched structures, we changed to an inductively coupled plasma-reactive ion etching (ICP-RIE) process. We used SF_6 and also CHF_3 based on our results above and since it is reported that CHF_3 is superior to CF_4 in dry etching of LN due to suppressed deterioration of the surface.[3] SF_6 gas was used in experiment 3. CHF_3 gas was used in experiments 4 and 5, and argon was added in the chamber to enhance the physical

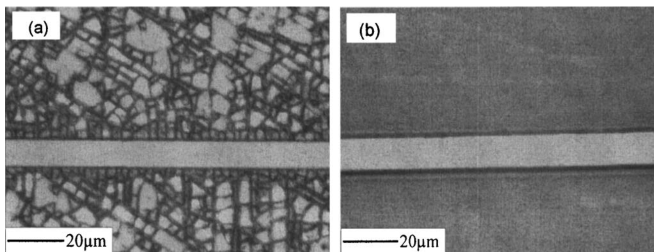

FIG. 1. Optical microscope images of the etched surface of PE-LN in different gases. The straight stripe was not etched because of Cr mask. (a) Etched with CF_4 (1). (b) Etched with SF_6 (2).

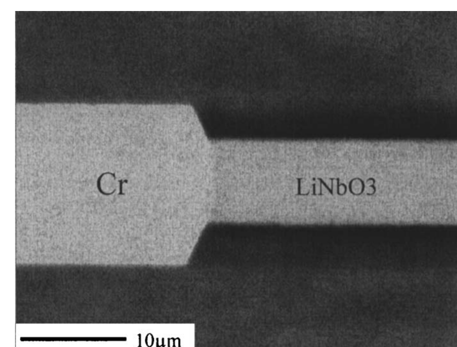

FIG. 2. PE-LN surface etched by SF_6 gas. On each side of the stripe, the under-etching rates are 3.5 and 4.0 μm/h, respectively.

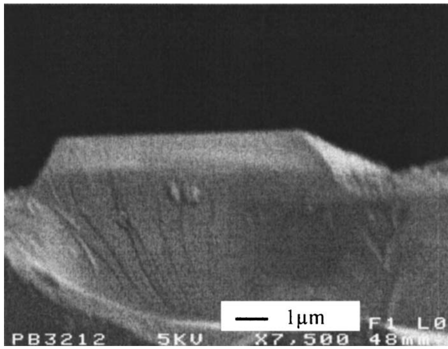

FIG. 3. SEM picture of end face of PE-LN etched by SF_6 gas. Asymmetric etching on two sides of the ridge structure is shown.

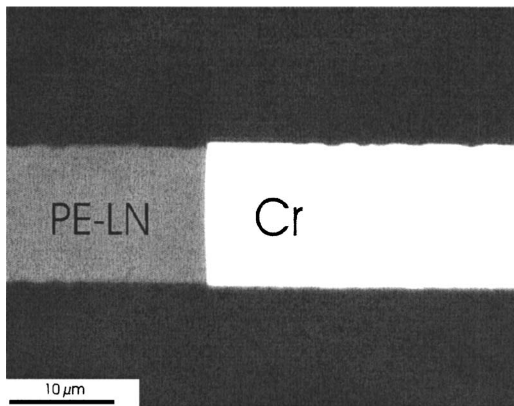

FIG. 4. PE-LN surface etched by CHF_3/Ar gas. The width of PE-LN stripe is almost the same as that of Cr, which indicates the reduced under-etching effect.

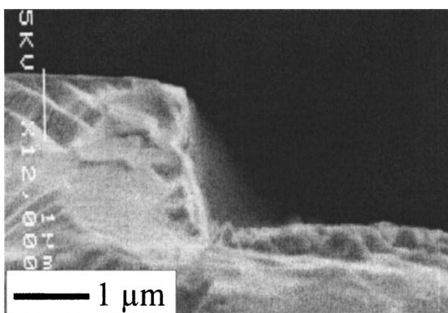

FIG. 5. SEM picture of end face of PE-LN etched by CHF_3/Ar gas; a nearly vertical etched wall is shown.

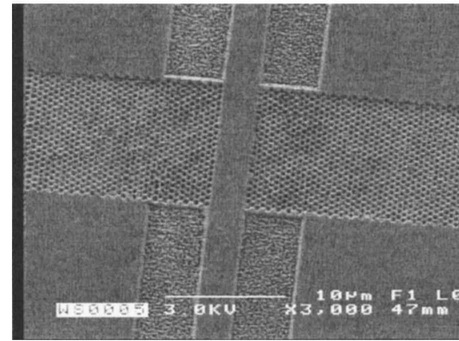

FIG. 6. SEM micrograph of a PE-LN photonic crystal waveguide. Interpore distance of the periodic pattern is 500 nm. Etching parameters are CHF_3/Ar etching gas, 1500 W ICP power, 130 V dc bias, 6 mTorr chamber pressure, and no substrate cooling.

component during etching. Since fully fluorinated niobium will also be formed in the etching process (NbF_5), which has its boiling point at about 234 °C,[11] we expect a substrate temperature dependence on the etching rate. The etching rate of PE-LN is 2.88 $\mu m/h$ with He-backside cooling keeping the sample temperature nominally at room temperature, while the etching rate was about 5.7 $\mu m/h$ without cooling (Table I). The selectivity of PE-LN to the Cr mask was 32:1. The etched surface of experiment 5 is shown in Fig. 4. The Cr stripe covered the PE-LN, and part of the Cr layer was peeled off to display the fabricated PE-LN stripe, shown in the left part of the picture. The width of PE-LN stripe is nearly the same as that of Cr, which means that the under etching is greatly reduced. In experiment 5, a nearly vertical etched wall is obtained with an angle of 82° (Fig. 5). In literature, mainly parallel plate RIE based plasma based on CHF_3 is applied. The reported etching rates are 0.4 $\mu m/h$ for pure LN and 0.6 $\mu m/h$ for proton-exchanged LN with strongly rounded side walls of the trenches.[9] We also performed etching of complex photonic crystal waveguide structures using the etching recipe 5. The diameter of the pore is 340 nm while the periodicity is 500 nm, and the etching depth measured in ridge waveguide region is about 1.5 μm. First etching results are shown in Fig. 6.

IV. CONCLUSION

In conclusion, we tested different plasma-chemical etching processes to etch proton-exchanged $LiNbO_3$. We obtained for dry etching with SF_6 gas at a gas chamber pressure 500 mTorr: PE-LN was etched at about 1.5 $\mu m/h$ while pure LN could not be etched. Due to the high pressure, nearly isotropic etching was observed. The selectivity of PE-LN to the Cr mask was 46:1. Using ICP-RIE etching, negligible under etching and nearly vertical etched walls on PE-LN samples were obtained applying CHF_3/Ar gas at a chamber pressure of 6 mTorr. The etching rate of PE-LN is about 5.7 $\mu m/h$, and the selectivity of PE-LN to the Cr mask was 32:1. This compares to literature values of PE-LN of about 0.6 $\mu m/h$. First photonic crystal waveguide structures with a lattice constant of 500 nm have been successfully fabricated with etching depth of about 1.5 μm.

ACKNOWLEDGMENTS

One of the authors (H.H.) thanks for the financial support from the Alexander von Humboldt Foundation.

[1] W. Sohler, Thin Solid Films **175**, 191 (1989).
[2] J. G. Scott, A. J. Boyland, S. Mailas, C. Grivas, O. Vagner, S. Lagoutte, and W. Eason, Appl. Surf. Sci. **230**, 138 (2004).
[3] N. Mitsugi, H. Nagata, K. Shima, and M. Tamai, J. Vac. Sci. Technol. A **16**, 2245 (1998).
[4] D. M. Manos and D. L. Flamm, *Plasma Etching: An Introduction* (Academic, New York, 1989), p. 476.
[5] H. Nagata, N. Mitsugi, K. Shima, M. Tamai, and E. M. Haga, J. Cryst. Growth **187**, 573 (1998).
[6] M. Tamura and S. Yoshikado, Surf. Coat. Technol. **169–170**, 203 (2003).
[7] O. Espeso, G. Garcia, A. Climent, F. Agullo-Lopez, G. De la Paliza, J. M. Cabrera, and T. Sajavaara, J. Appl. Phys. **94**, 7710 (2003).
[8] V. Fedorov, Y. Korkishko, A. Alkaev, and E. Maslennikov, Proceedings of the 11th European Conference on Integrated Optics (ECIO'03), Prague, 2003, Vol. 1, p. 385.
[9] V. Foglietti, E. Cianci, D. Pezzetta, C. Sibilia, M. Marangoni, R. Osellame, and R. Ramponi, Microelectron. Eng. **67–68**, 742 (2003).
[10] A. P. Milenin, C. Jamois, R. B. Wehrspohn, and M. Reiche, Microelectron. Eng. **77**, 139 (2005).
[11] www.webelements.com